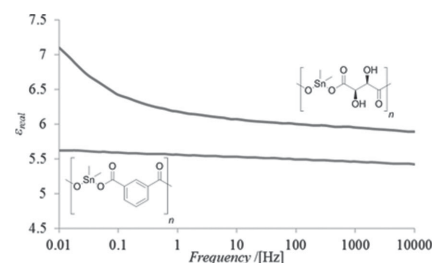


# Effect of Incorporating Aromatic and Chiral Groups on the Dielectric Properties of Poly(dimethyltin esters)

Aaron F. Baldwin, Rui Ma, Tran Doan Huan, Yang Cao,  
Ramamurthy Ramprasad, Gregory A. Sotzing\*

High-dielectric constant materials are critical for numerous applications such as photovoltaics, photonics, transistors, and capacitors. There are numerous polymers used as dielectric layers in these applications but can suffer from having a low dielectric constant, small band gap, or ferroelectricity. Here, the structure–property relationship of various poly(dimethyltin esters) is described that look to enhance the dipolar and atomic polarization component of the dielectric constant. These polymers are also modeled using first principles calculations based on density functional theory (DFT) to predict such values as the total, electronic, and ionic dielectric constant as well as structure. A strong correlation is achieved between the theoretical and experimental values with the polymers exhibiting dielectric constants  $>4.5$  with dissipation on the order of  $10^{-3}$ – $10^{-2}$ .



## 1. Introduction

Research into next-generation dielectric/insulating materials has grown exponentially due to their use in a plethora of applications such as photovoltaics, transistors, photonics, and capacitors.<sup>[1–5]</sup> Consequently, the development of a dielectric material that can either fulfill the requirements across multiple applications or a number of devices within

one type is ideal. Polymers are intriguing materials as dielectrics as they allow for easier processing techniques and lower densities versus inorganics leading to the formation of lightweight, flexible films, and making them suitable for devices in which size and space are limited.

However, compared to inorganic materials, organic polymers exhibit much lower dielectric constants as a result of either a minute or nonexistent contribution of the ionic component to the total dielectric constant.<sup>[6]</sup> To increase the dielectric constant of polymers, two methods are commonly employed. The first aims to increase the ionic contribution through the addition of permanent dipoles (dipolar polarization) either within the polymer backbone or as pendant groups. This has led to much research into such polymer structures such as polyimides, polyureas, functionalized polyolefins, and halogenated homo- and copolymers.<sup>[7]</sup> The increase in dielectric constant of these materials can also lead to a reduction in band gap and/or breakdown strength or in the case of the polyvinylidene fluoride (PVDF) ferroelectric behavior.<sup>[8]</sup> The second method incorporates high-dielectric constant

Dr. A. F. Baldwin, R. Ma, Prof. G. A. Sotzing  
Polymer Program, Institute of Materials Science, University  
of Connecticut, 97 North Eagleville Rd Storrs, CT 06269, USA  
E-mail: g.sotzing@uconn.edu

Dr. T. D. Huan, Prof. R. Ramprasad  
Department of Materials Science and Engineering,  
Institute of Materials Science, University of Connecticut,  
97 North Eagleville Rd Storrs, CT 06269, USA

Prof. Y. Cao  
Department of Electrical and Computer Engineering,  
University of Connecticut, 97 North Eagleville Rd Storrs,  
CT 06269, USA

inorganic nanofillers, such as barium titanate, which in addition may also give rise to interfacial polarization between the polymer matrix and nanoparticle.<sup>[9]</sup> In order to achieve a total increase in dielectric constant, a large portion of the higher density nanoparticle needs to be added, which can cause detrimental effects to other electronic properties of the polymer such as reduced breakdown strength.<sup>[10]</sup> Experiments have shown that even the dielectric constant of the nanoparticle is related to its size and that the smaller the size of the nanoparticle a much lower dielectric constant is observed.<sup>[11]</sup>

Recent computations have shown the benefit of the incorporation of metal atoms, such as tin, covalently bonded within a polymer backbone on the dielectric properties.<sup>[12,13]</sup> By imbedding the metal atom into the polymer, it is expected that undesirable effects due to aggregation will be absent and that the metal will be dispersed throughout the matrix. Also, creating polymers containing tin-heteroatom, such as oxygen, bonds leads to an enhancement of the dipolar and atomic polarization due to the increase in electronegativity difference between the two compared with carbon-heteroatom. We recently studied the structure–dielectric property relationship of aliphatic poly(dimethyltin esters) where dimethyltin dicarboxylate groups were joined together with methylene groups of varying length.<sup>[14,15]</sup> These polymers exhibited dielectric constants  $\geq 5.3$ , dielectric loss for the majority of the systems on the order of  $10^{-2}$  and band gaps  $\geq 4.6$  eV. Based on these results, the critical amount of tin within a polymer, dependent upon the requirements of the application, can be identified. It was found theoretically and confirmed experimentally that the coordination complex and polymer structure, and as a result the dielectric properties, could be tailored by using different processing methods.

Here, we investigate a series of poly(dimethyltin esters), based on the synthetic method described by Zilkha and Carraher, in which the effect of having an aromatic ring adjacent to the dimethyltin dicarboxylate group or chiral centers on polymer morphology, thermal stability, and dielectric properties.<sup>[16]</sup> We employ density functional theory (DFT) to model our polymers and calculate the resulting dielectric properties and compare to the experimental results.<sup>[17]</sup> We can conclude from these results which type of aromatic ring, i.e., electron donating or withdrawing, positioning of the dimethyltin dicarboxylate group on the aromatic ring and the level of crystallinity needed to optimize the dielectric properties of these polymers. Furthermore, based on these correlations, it is implied that the modelling method is effective in the design of dielectric materials and from this a fundamental understanding of how to improve these materials, possibly incorporating both types of functionalities, for a second generation can be achieved.

## 2. Experimental Section

### 2.1. Theoretical Methodology

Our DFT calculations were performed using Vienna Ab initio Simulation Package (VASP), employing the Perdew-Burke-Ernzerhof (PBE) functional for the exchange-correlation energies and the non-local vdW-DF2 for the long-range van der Waals interactions.<sup>[18–20]</sup> To determine the structures of the examined aromatic and chiral poly(dimethyltin esters), we used the minima-hopping structure prediction method.<sup>[21]</sup> Given that the polymer structures are predicted, we computed the relevant properties, one of which is the band gap at the PBE level. The dielectric constants were also calculated within the formalism of density functional perturbation theory as implemented in VASP.<sup>[22]</sup>

### 2.2. Materials

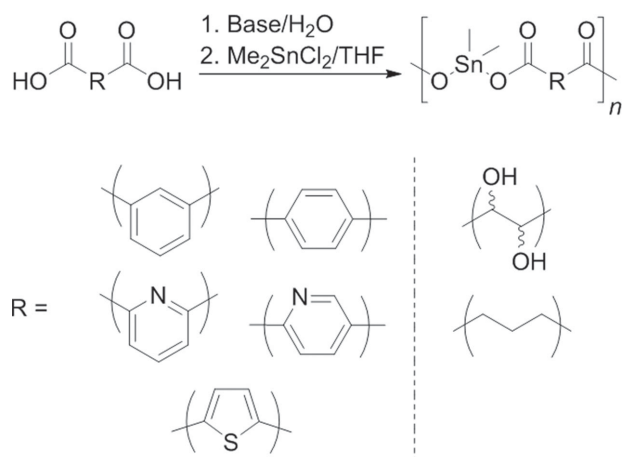
All diacids (Acros Organics), dimethyltin dichloride (TCI), and tetrahydrofuran (J.T. Baker, HPLC grade) were used as received. Sodium hydroxide, NaOH, and triethylamine, TEA, were purchased from Fisher Scientific. Deionized water was obtained from a Millipore purification system.

### 2.3. Instrumentation

Fourier transform infrared (FTIR) spectra were collected using a Nicolet Magna 560 FTIR spectrometer (resolution  $0.35\text{ cm}^{-1}$ ) and are reported in wavenumbers ( $\text{cm}^{-1}$ ). The spectrum was obtained from a KBr pellet containing the polymer. Thermogravimetric analysis (TGA) was performed using a TA instruments TGA Q500 with a heating rate of  $10\text{ }^\circ\text{C min}^{-1}$  under  $\text{N}_2$  atmosphere. Differential scanning calorimetry (DSC) was performed on a TA instruments DSC Q series with a first heating cycle rate of  $40\text{ }^\circ\text{C min}^{-1}$ , a cooling cycle of  $40\text{ }^\circ\text{C min}^{-1}$ , and a second heating cycle of  $10\text{ }^\circ\text{C min}^{-1}$ . Dielectric data were collected using an IMASS time domain dielectric spectrometer (TDS) with measurements done in an air-circulating oven at constant temperature. X-ray diffraction (XRD) data were collected on powdered samples using a Bruker D2 Phaser with a  $\text{Cu-K}\alpha$  ( $\lambda = 1.54184\text{ \AA}$ ) radiation source.

### 2.4. Synthesis

Scheme 1 illustrates the general reaction procedure for the synthesis of poly(dimethyltin esters). In general, to a round bottomed flask is added the diacid(s) and distilled water. To this aqueous solution/mixture is added slightly more than two equivalents, versus the diacid, of either NaOH, in the case of the aromatic polymers, or TEA, for the tartaric acid systems, to create an acid/base equilibrium and allow for carboxylation. The aqueous solution is then stirred rapidly. To a second flask is added slightly lower molar equivalent versus the diacid of dimethyltin dichloride and dissolved in THF. The organic phase is then rapidly added to the aqueous phase. The solution is stirred until the polymer precipitates from the interface. The solid is filtered and washed with equal amounts of THF and water and dried in vacuo (30 in. Hg) at  $115\text{ }^\circ\text{C}$  for 24 h (see Supporting Information for synthesis details).



**Scheme 1.** Interfacial polymerization reaction scheme for the formation of poly(dimethyltin esters).

### 3. Results and Discussion

#### 3.1. Coordination Complexes of Poly(dimethyltin esters)

Tin compounds have been reported to take a coordination number of four, five, six, or seven. From our calculations, the poly(dimethyltin esters) are six coordinated, forming octahedral complexes, which are grouped into three different structural motifs, herein labeled the  $\alpha$ -,  $\beta$ -, and  $\gamma$ -motif (see Supporting Information for pictorial representation for these structures). The  $\alpha$ -motif represents a 1D, intrachain complex in which the tin atom is covalently bonded to two oxygen atoms from the two carboxylate groups and coordinated with two longer bonds to the two carbonyl oxygen atoms from the same repeat unit. In contrast, the  $\beta$ -motif is a 3D, interchain structure characterized by the same two covalent Sn-O bonds but with coordination occurring with carbonyl oxygen atoms from a different polymer chain. The  $\gamma$ -motif is the combination of the  $\alpha$ - and  $\beta$ -motif within the same polymer chain, shown

to be on the same repeat unit, i.e., one carboxylate being intrachain and the other interchain; though in reality, the polymer chain is a mixture of both complexes in an unknown ratio.

Experimentally, the presence of these three motifs is confirmed using IR (see Supporting Information for IR spectra of the polymers). Though Peruzzo was the first to hypothesize that the two complexes could coexist, Carraher was the first to report the IR absorption range of these complexes.<sup>[23,24]</sup> The complexes are characterized by asymmetric and symmetric bridging (interchain), 1550–1580  $\text{cm}^{-1}$  and 1410–1430  $\text{cm}^{-1}$ , respectively, and nonbridging (intrachain), 1635–1660  $\text{cm}^{-1}$  and 1350–1370  $\text{cm}^{-1}$ , respectively, carbonyl absorptions. Each of these absorptions is present in the IR spectra of the polymers described here in varying intensities. This confirms what is expected, that at ambient conditions each of the motifs exists in an unknown quantity within the polymer chains.

#### 3.2. Aromatic Poly(dimethyltin esters)

As stated previously, three different types of aromatic systems are investigated, electron-withdrawing pyridine, electron-donating thiophene, and electron “neutral” benzene rings. The effect of the placement of the carboxylic acids in relation to each other on both the pyridine and benzene systems on the dielectric properties is also evaluated. A second dipole is observed when the carboxylic acids are metapositioned to each other versus parapositioned. Due to the insolubility in most common organic solvents, pellets were pressed to measure the dielectric properties. The dielectric properties (Table 1) at ambient conditions, ca. 25 °C and 1 atm, illustrated in Figure 1(a and b), show consistent dielectric constants over a frequency range of  $10^{-2}$ – $10^4$  Hz. As expected the three polymers, poly(dimethyltin isophthalate) (p(DMTIso)),

**Table 1.** Theoretical and experimental dielectric properties of poly(dimethyltin esters).

Polymer	$\epsilon_{\text{exp.}}^{\text{a)}$	$\epsilon_{\text{DFT}}^{\text{b)}$	$\tan\delta$ [%]
p(DMTIso)	5.52	5.90	0.39
p(DMTTer)	4.71	6.19	3.13
p(DMT 2,6-DPA)	5.64	6.79	1.50
p(DMT 2,5-DPA)	4.81	6.30	1.04
p(DMT 2,5-TDC)	5.08	7.91	3.04
p(DMT D-Tar)	6.18	7.15	3.13
p(DMT 50/50 Glu/D-Tar)	5.31	6.32	1.08
p(DMT 50/50 Glu/L-Tar)	5.55	–	1.95
p(DMT 50/50 Glu/DL-Tar)	4.97	6.52	5.33

<sup>a)</sup>Average value over  $10^{-2}$ – $10^4$  Hz; <sup>b)</sup>Theoretical values based on density functional theory (DFT).

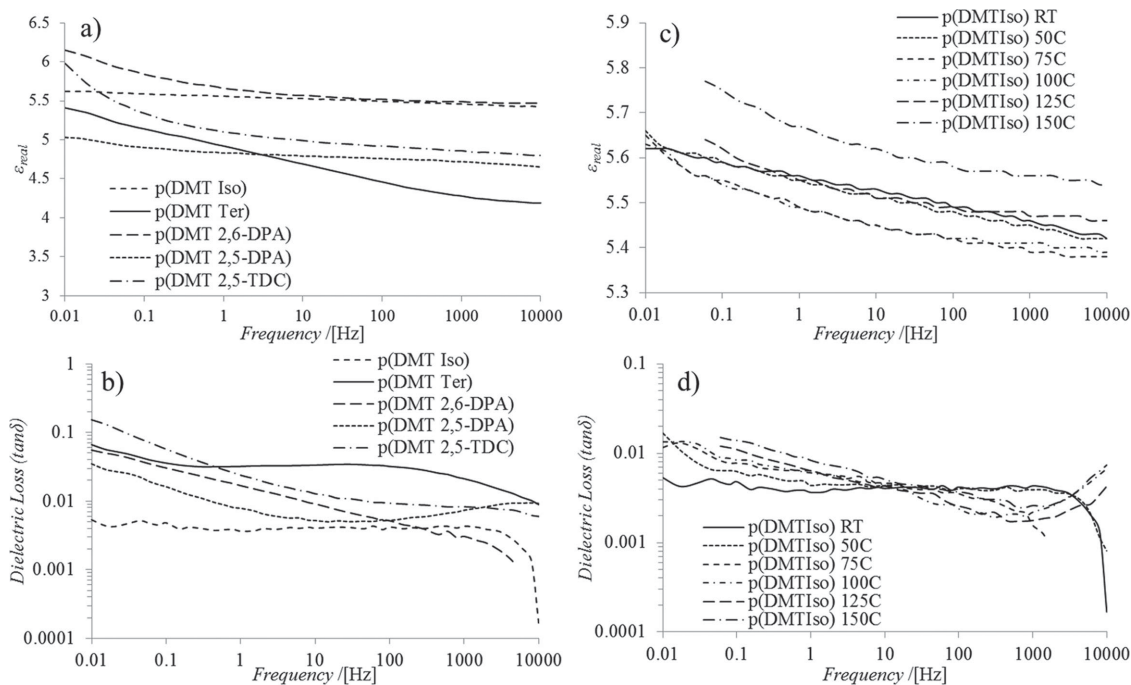


**Figure 1.** Dielectric properties (a and b) of poly(dimethyltin isophthalate), p(DMTIso); poly(dimethyltin terephthalate), p(DMTTer); poly(dimethyltin 2,6-dipicolinate), p(DMT 2,6-DPA); poly(dimethyltin 2,5-dipicolinate), p(DMT 2,5-DPA); and poly(dimethyltin 2,5-thiophenedicarboxylate), p(DMT 2,5-TDC), at ambient conditions. Temperature dependence of dielectric properties, c and d, of p(DMTIso).

poly(dimethyltin 2,6-dipicolinate) (p(DMT 2,6-DPA)), poly(dimethyltin 2,5-thiophenedicarboxylate) (p(DMT 2,5-TDC)), in which the carboxylic acids are metapositioned exhibit higher average dielectric constants ( $\epsilon_{\text{avg}}$ ), 5.52, 5.64, and 5.08, respectively. In contrast, poly(dimethyltin terephthalate) (p(DMTTer)) and poly(dimethyltin 2,5-dipicolinate) (p(DMT 2,5-DPA)) have  $\epsilon_{\text{avg}}$  values of 4.71 and 4.81, respectively. The trend in dielectric constant for the metapositioned polymers, when comparing what type of aromatic ring is present, is pyridine > benzene > thiophene. The behavior of the experimental dielectric constants reported for the metapositioned carboxylate groups is a result of the size and electron density/polarity of the aromatic ring. It is expected that as the size of the ring system is increased the resulting dielectric constant would be lower due to larger molecular volume. However, thiophene is electron rich and pyridine is electron deficient, which gives rise to differences in electron density within the ring system. For example, the electron density of the benzene ring is spread evenly, whereas the in the pyridine ring, the electron density is localized around the nitrogen. As for the parapositioned polymers, the benzene containing polymer, p(DMTTer), has a higher average dielectric constant versus the pyridine, p(DMT 2,5-DPA), though there is an inflection point at 3 Hz and the pyridine containing polymer exhibits a higher dielectric constant. Again the behavior in the data can be attributed to the polarity of the aromatic ring system.

The calculated dielectric constants show that p(DMT 2,5-TDC) has the highest dielectric constant followed by the pyridine- and benzene-based polymers. In the pyridine polymers, the metapositioned polymer has a higher dielectric constant than the parapositioned, which is the opposite for the benzene-based systems. The lack of correlation in trends can be attributed to the calculations being performed on highly crystalline systems at temperatures below ambient conditions as well as complications in the experimental measurements with respect to sample preparation and consistency of measurements. This also highlights the fact that the exact structures of these polymers are quite complex versus other systems we have investigated and that further experimental data are required to pinpoint further details of polymer morphology for input into our models.

The performance of a dielectric material is also governed by its dielectric loss/dissipation. Minimal loss is ideal as high dissipation in dielectric constant will result in energy absorption or in the case of photonic crystals a variation in band gap as it is inversely proportional to dielectric constant.<sup>[5]</sup> All of the polymers have dissipation factors at or below 3%, with p(DMTIso) having an average dissipation of 0.39%. The high dissipation for the polymers can be attributed to presence of residual water, which is seen in the TGA analysis (see Supporting Information for TGA traces).

The incorporation of aromatic rings also serves to increase the thermal stability of the polymers as a result of the increase in the rigidity of the polymer and the number of bonds that need to be broken, in the case of aromatic systems two 1.5 bonds need to be broken in order for scission of the polymer chain to occur. The aromatic polymers are all stable to temperatures  $>250\text{ }^{\circ}\text{C}$  with increased degradation rate not occurring until ca.  $300\text{ }^{\circ}\text{C}$ . As highlighted in the previous paragraph, p(DMTIso) exhibits a dielectric constant of 5.52 with a dissipation well below 1%. Therefore, temperature dependence on the dielectric properties of this polymer was looked at further (Figure 1c,d). As the temperature is increased, the dielectric constant is lowered due to the removal of residual solvent and at temperatures  $\geq 125\text{ }^{\circ}\text{C}$ , the dielectric constant is enhanced as a result of heightened thermal energy allowing the dipoles to align faster to the applied electric field. As expected, the dissipation factor increases with temperature due to thermal loss resulting from friction caused from the movement of polymer chains. Fortunately, the dissipation remains below 1% for much of the frequency range. However, at elevated temperatures, exposure to air may cause oxidation resulting in electrical breakdown at these temperatures. The conditions of these experiments, therefore, were run in order to mimic dielectric materials used in

applications where they may be exposed oxygen in the air and it is expected that this represents the worst case scenario and further testing in an inert environment would lead to enhancement of the dielectric properties. It is hoped that by increasing the maximum operating temperature the emphasis on device cooling will be less stringent.

### 3.3. Chiral Center Containing Poly(dimethyltin esters)

Controlling the crystallinity of polymers has been shown both theoretically and experimentally to have effects on the electronic properties of polymers. Sun et al. have carried out calculations on crystalline and amorphous materials that show amorphous polymers have higher breakdown strength due to the absence of cavities in which charge can accumulate and migrate from and which are inherent in highly crystalline materials.<sup>[25]</sup> Wu et al., in their paper describing the synthesis and characterization of an amorphous polythiourea, relate the improvement in conduction loss to random dipoles in the amorphous material causing stronger scattering of charge carriers.<sup>[71]</sup> In our systems, we can control crystallinity by employing a diacid that contains chiral centers, in this case tartaric acid. The D- and L- forms of tartaric acid lead to more amorphous materials since chain packing is disrupted due to the two

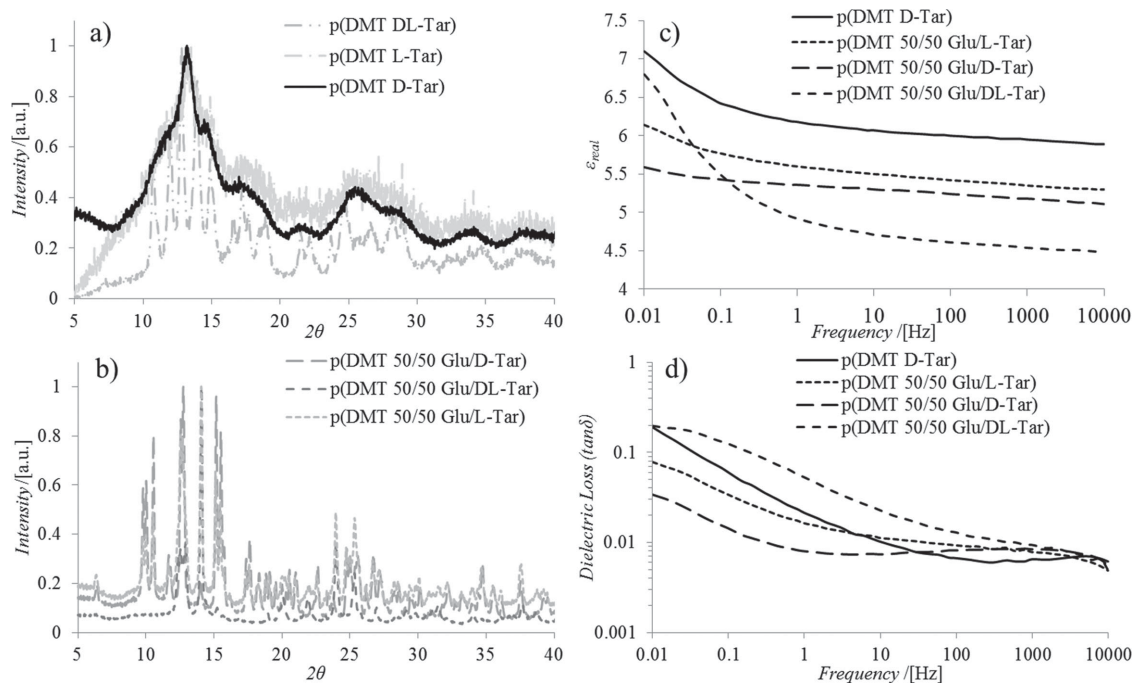


**Figure 2.** XRD patterns of homopolymers (a) of poly(dimethyltin esters) based on D-, L-, and a racemic mixture of D- and L-tartaric acid, p(DMT D-Tar), p(DMT L-Tar), and p(DMT DL-Tar), respectively. XRD patterns of copolymers (b) of poly(dimethyltin esters) using a 50/50 feed ratio of glutaric acid/tartaric acid, p(DMT 50/50 Glu/D-Tar), p(DMT 50/50 Glu/L-Tar), and p(DMT 50/50 Glu/DL-Tar). Dielectric properties (c and d) of p(DMT D-Tar), p(DMT 50/50 Glu/D-Tar), p(DMT 50/50 Glu/L-Tar), and p(DMT 50/50 Glu/DL-Tar) at ambient conditions.

hydroxyl groups being in the same plane. A more crystalline polymer can be synthesized by using some mixture of the enantiomers, in this case the racemate, since tighter chain packing can be achieved. This is confirmed through XRD, Figure 2a, which show a broad diffraction pattern for poly(dimethyltin D-tartrate) (p(DMT D-Tar)) and poly(dimethyltin L-tartrate) (p(DMT L-Tar)) compared to the more well-defined diffraction pattern of poly(dimethyltin DL-tartrate) (p(DMT DL-Tar)). The hydroxyl groups also serve to enhance chain–chain interaction as a result of the possibility for hydrogen bonding between -OH groups or the coordination of the electron lone pairs with the tin atom in competition with the carbonyl oxygen atom. Copolymers of glutaric acid with the various tartaric acid enantiomers were also synthesized to see if crystallinity and coordination complexes could be tailored. The XRD patterns, Figure 2b, of these copolymers show that the polymers using 50/50 feed ratios of the diacids are crystalline in nature.

Pellets were pressed in order to compare the dielectric properties of the polymers (Figure 2c,d). As expected the homopolymer, p(DMT D-Tar), had a higher dielectric constant,  $\epsilon_{\text{avg}}$  of 6.18, compared to the copolymers as a result of the higher volume of dipoles per unit. Unfortunately, p(DMT DL-Tar) could not be tested as the pellet easily crumbled. This could be due to p(DMT DL-Tar) being lower in molecular weight compared to p(DMT D-Tar) though this was not confirmed. Pellets of the copolymers showed that the incorporation of the amorphous tartaric acid led to a higher dielectric constant, 5.31 and 5.55 for D-Tar- and L-Tar-based systems, respectively, versus 4.97 for the DL-Tar system. The dissipation of the polymers is higher than the aromatic systems, >1% for all polymers with p(DMT 50/50 Glu/DL-Tar) having a dissipation >5%. However, it is shown that using an enantiomerically pure tartaric acid, which can impart more amorphous regions within the matrix, is more beneficial as the dissipation/conduction loss of these copolymers is about five times lower than of the copolymer containing the racemic mixture of D- and L-tartaric acid. The theoretical calculations also show the p(DMT D-Tar) to have a higher dielectric constant versus the copolymers, though the more crystalline p(DMT 50/50 Glu/DL-Tar) has a higher dielectric constant compared to the other two copolymers. Again this can be attributed to the calculations being done on fully crystalline systems, whereas it is known that there is some semicrystalline nature in these polymers.

## 4. Conclusion

In summary, we have shown the effect of two different variables, aromaticity and chirality, on the dielectric properties of poly(dimethyltin esters), which may be employed in a number of applications where a dielectric layer is

required. All of the polymer systems exhibit dielectric constants >4.5 with dissipation between 0.1% and 10%. From these results, it is shown that having an aromatic ring improves the thermal stability of these polymers and that the nature of the ring is not as critical to the dielectric properties as the positioning on the ring of the dimethyltin dicarboxylate is. Also, incorporating diacids that can impart a more amorphous nature into the polymer chain are beneficial to the dielectric properties. This work included the use of state-of-the-art calculations at the level of DFT to model the polymer structures and from these configurations predict the resulting dielectric constants. There is a good correlation between theoretical and experimental results but some work still needs to be done due to the highly complex coordination complexes that are formed. However, based on these observations, we now have the knowledge to improve upon these materials, possibly having both functionalities present in the polymer backbone, for a second generation.

## Supporting Information

Supporting Information is available from the Wiley Online Library or from the author.

Acknowledgements: This work was supported by a Multi-University Research Initiative (MURI) grant from the Office of Naval Research, under award number N00014-10-0944. The authors thank JoAnne Ronzello for performing all dielectric measurements, Maximilian Amsler, and Stefan Goedecker for making available the minima-hopping method code.

Received: September 9, 2014; Revised: October 7, 2014;  
Published online: November 10, 2014; DOI: 10.1002/marc.201400507

Keywords: density function theory (DFT); dielectric properties; organometallic polymers; structure–property relations; X-ray diffraction (XRD)

- [1] a) P. M. Hergenrother, *High Perform. Polym.* **2003**, *15*, 3; b) V. K. Thakur, M. R. Kessler, in *Advance Energy Materials*, Vol. 1 (Eds: A. Tiwari, S. Valyukh), Scrivener Publishing, Beverly, MA, USA **2014**, Ch. 5.
- [2] a) Y.-G. Ha, K. Everaerts, M. C. Hersam, T. J. Marks, *Acc. Chem. Res.* **2014**, *47*, 1019 ; b) T. Diekmann, U. Hilleringmann, in *Physical and Chemical Aspects of Organic Electronics*, Vol. 1 (Ed: C. Wöll), Wiley-VCH, Weinheim, Germany **2009**, Ch. 18.
- [3] G. M. Rebeiz, in *RF MEMS: Theory, Design, and Technology*, Wiley, Hoboken, NJ, USA **2003**.
- [4] N. Camaioni, R. Po, *J. Phys. Chem. Lett.* **2013**, *4*, 1821.
- [5] W. Zhou, V. Nair, G. Thiruvengadam, in *Photonic Crystal Materials and Devices IV. Proc. of SPIE*, Vol. 6128 (Eds: A. Adibi, S.-Y. Lin, A. Scherer), SPIE, Bellingham Washington **2006**, 61280B(1-8).
- [6] a) C. C. Wang, G. Pilania, S. A. Boggs, S. Kumar, C. Breneman, R. Ramprasad, *Polymer* **2014**, *55*, 979; b) V. Sharma,

- C. C. Wang, R. G. Lorenzini, R. Ma, Q. Zhu, D. W. Sinkovits, G. Pilania, A. R. Oganov, S. Kumar, G. A. Sotzing, S. A. Boggs, R. Ramprasad, *Nat. Commun.* **2014**, *5*, 4845.
- [7] a) M. Zhang, X. Yuan, L. Wang, T. C. M. Chung, T. Huang, W. de Groot, *Macromolecules* **2014**, *47*, 571; b) T. C. M. Chung, *Green Sustainable Chem.* **2012**, *2*, 29; c) W. W. Yager, W. O. Baker, *J. Am. Chem. Soc.* **1942**, *64*, 2164; d) W. O. Baker, W. W. Yager, *J. Am. Chem. Soc.* **1942**, *64*, 2171; e) I. Bacosca, M. Bruma, T. Koepnick, B. Schull, *J. Polym. Res.* **2013**, *20*, 53; f) J. Pan, K. Li, J. Li, T. Hsu, Q. Wang, *Appl. Phys. Lett.* **2009**, *95*, 022902; g) J. Pan, K. Li, S. Chuayprakong, T. Hsu, Q. Wang, *ACS Appl. Mater. Interfaces* **2010**, *2*, 1286; h) S. Tasaka, K. Ohishi, N. Inagaki, *Ferroelectrics* **1995**, *171*, 203; i) S. Wu, W. Li, M. Lin, Q. Burlingame, Q. Chen, A. Payzant, K. Xiao, Q. M. Zhang, *Adv. Mater.* **2013**, *25*, 1734; j) C. -G. Duan, W. N. Mei, J. R. Hardy, S. Ducharme, J. Choi, P. A. Dowben, *Europhys. Lett.* **2003**, *61*, 81; k) B. Chu, X. Zhou, K. Ren, B. Neese, M. Lin, Q. Wang, F. Bauer, Q. M. Zhang, *Science* **2006**, *313*, 334; l) X. Zhou, B. Chu, B. Neese, M. Lin, Q. M. Zhang, *IEEE Trans. Dielectrics Electrical Insulation* **2007**, *14*, 1133; m) A. F. Baldwin, R. Ma, C. C. Wang, R. Ramprasad, G. A. Sotzing, *J. Appl. Polym. Sci.* **2013**, *22*, 699; n) R. Ma, A. F. Baldwin, C. C. Wang, I. Offenbach, M. Cakmak, R. Ramprasad, G. A. Sotzing, *ACS Appl. Mater. Interfaces* **2014**, *6*, 10443.
- [8] J. A. Chilton, *Plastics for Electronics*, (Ed: M. Goosey), Springer, New York **1999**, 243.
- [9] a) J. Y. Li, L. Zhang, S. Ducharme, *Appl. Phys. Lett.* **2007**, *90*, 132901; b) D. Q. Tan, Q. Chen, P. Irwin, Y. U. Wang, *IEEE Trans. Ultrasonic Ferroelectrics, Frequency Control* **2013**, *60*, 1619; c) H. Zhao, R. K. Y. Li, *Compos: Part A* **2008**, *39*, 602.
- [10] Z. M. Dang, J. -K. Yuan, S. -H. Yao, R. -J. Liao, *Adv. Mater.* **2013**, *25*, 6334.
- [11] X. Hao, *Adv. Dielectrics* **2013**, *3*, 1330001.
- [12] G. Pilania, C. C. Wang, K. Wu, N. Sukumar, C. Breneman, G. A. Sotzing, R. Ramprasad, *J. Chem. Inf. Model.* **2013**, *53*, 879.
- [13] G. Pilania, C. C. Wang, X. Jiang, S. Rajasekaran, R. Ramprasad, *Sci. Rep.* **2013**, *3*, 2810.
- [14] A. F. Baldwin, R. Ma, A. Mannodi-Kanakkithodi, T. D. Huan, C. C. Wang, M. Tefferi, J. E. Marszalek, M. Cakmak, Y. Cao, R. Ramprasad, G. A. Sotzing, unpublished.
- [15] A. F. Baldwin, T. D. Huan, R. Ma, A. Mannodi-Kanakkithodi, M. Tefferi, N. Katz, Y. Cao, R. Ramprasad, G. A. Sotzing, unpublished.
- [16] a) M. Frankel, D. Gertner, D. Wagner, A. Zilkha, *J. Appl. Polym. Sci.* **1965**, *9*, 3383; b) S. Migdal, D. Gertner, A. Zilkha, *J. Organomet. Chem.* **1968**, *11*, 441; c) C. E. Carraher Jr., R. L. Dammeier, *J. Polym. Sci., Part A* **1972**, *10*, 413.
- [17] a) P. Hohenberg, W. Kohn, *Phys. Rev.* **1964**, *136*, B864; b) W. Kohn, L. Sham, *Phys. Rev.* **1965**, *140*, A1133.
- [18] a) G. Kresse, J. Hafner, *Phys. Rev. B* **1993**, *47*, 558; b) G. Kresse, *PhD thesis*, Technische Universität Wien, Austria, **1993**; c) G. Kresse, J. Furthmüller, *J. Comput. Mater. Sci.* **1996**, *6*, 15; d) G. Kresse, J. Furthmüller, *Phys. Rev. B* **1996**, *54*, 11169.
- [19] J. P. Perdew, K. Burke, M. Ernzerhof, *Phys. Rev. Lett.* **1996**, *77*, 3865.
- [20] K. Lee, É. D. Murray, L. Kong, B. I. Lundqvist, D. C. Langreth, *Phys. Rev. B* **2010**, *82*, 081101(R).
- [21] a) S. Goedecker, *J. Chem. Phys.* **2004**, *120*, 9911; b) M. Amsler, S. Goedecker, *J. Chem. Phys.* **2010**, *133*, 224104.
- [22] S. Baroni, S. de Gironcoli, A. Dal Corso, *Rev. Mod. Phys.* **2001**, *73*, 515.
- [23] a) G. Plazzogna, V. Peruzzo, G. Tagliavini, *J. Organomet. Chem.* **1969**, *16*, 500; b) V. Peruzzo, G. Plazzogna, G. Tagliavini, *Organomet. Chem.* **1969**, *18*, 89; c) V. Peruzzo, G. Plazzogna, G. Tagliavini, *Organomet. Chem.* **1970**, *24*, 347; d) V. Peruzzo, G. Plazzogna, G. Tagliavini, *Organomet. Chem.* **1972**, *40*, 129.
- [24] C. E. Carraher Jr., *Angew. Makromol. Chem.* **1973**, *31*, 115.
- [25] Y. Sun, S. A. Boggs, R. Ramprasad, presented at *2013 IEEE Inter. Conf. on Solid Dielectrics*, Bologna, Italy, **2013**, 611.